ChemPubSoc Europe

DOI: 10.1002/ejic.201700716

EurJIC European Journal of Inorganic Chemistry

Full Paper

Layered Double Hydroxides

Electronic-Structure Calculations of Cation-Ordered II-III Layered Double Hydroxides: Origin of the Distortion of the Metal-Coordination Symmetry

K. Jayanthi,[a] P. Vishnu Kamath,[a] and Ganga Periyasamy*[a]

Abstract: Cation ordering brings down the crystal symmetry and introduces distortion into the coordination polyhedra around the divalent cations. In particular, edge sharing of the differently sized $[M(OH)_6]$ polyhedra causes a non-uniform distension of the array of hydroxy ions. The question arises as to whether this distortion has its origin in the Jahn–Teller distortion of metal coordination or a 2D "Peierls"-type distortion of the array of hydroxy ions. To address this question, DFT calculations were performed on the sulfate-intercalated [Cu–Cr], [Zn–Cr], and [Zn–Al] layered double hydroxides (LDHs). An analysis of the density of states shows that the distortion of the Cu^{2+} coordination polyhedron is due to the Jahn–Teller effect, whereas the Zn^{2+} coordination polyhedron in [Zn–Al] LDH likely suffers a "Peierls"-type distortion. In the [Zn–Cr] LDH, electronic-structure calculations do not predict any distortion in the metal coordination, which is in agreement with experimental results that show only a slight departure from ideal symmetry.

Introduction

Layered double hydroxides (LDHs) are widely used for a variety of applications, such as flame retardants, antacids, fillers for polymer composites, drug delivery, stabilizing agents in PVC,[1] and in optical devices.[2] They exhibit surface basicity, whereby they are used as solid-base catalysts for a wide range of base-catalyzed reactions.[3] They are also used for environmental amelioration on account of their excellent affinity and anion-uptake properties for chromates,[4] arsenates,[5] fluorides,[6] bromides,[7] and phosphates.[8] Given these applications, there is a crucial need to understand the electronic structure that underlies many of their unique properties.

The first step to understanding the electronic structure of a solid is knowledge of its crystal structure. The LDHs are obtained by isomorphous substitution of divalent ions by trivalent ions within a brucite-like structure of divalent hydroxides $M(OH)_2$. This results in a positively charged metal hydroxide layer of the composition $[M^{2+}_{1-x}M'^{3+}_{x}(OH)_2]^{x+}$. The value of x varies in the range $0.2 \le x \le 0.33$. The positive charge is compensated by the intercalation of anions in the interlayer. Since the LDHs are obtained from aqueous media, water molecules are also included in the interlayer gallery. The resulting compounds have the general formula $[M^{2+}_{1-x}M'^{3+}_{x}(OH)_2](A^{n-})_{x/n}\cdot yH_2O$ (A^{n-} = anion).[9] For the value of $x = 0.33$, the LDH composition is $[M_4M'_2(OH)_{12}](SO_4)\cdot nH_2O$ (n = 6.2–11.5 in this work). We abbreviate this by the symbol [M–M'].

There is a general understanding that the position of the trivalent M'^{3+} cation is disordered with respect to the divalent M^{2+} cation in the metal hydroxide layer. This implies that the M^{2+} and M'^{3+} cations occupy all of the six-coordinate sites within the metal hydroxide layer statistically. The layer can be treated as a (pseudo) single-cation hydroxide. Indeed, the a parameter of the LDHs matches that of the single-cation hydroxide, $Mg(OH)_2$ ($a_o \approx 3.10$ Å), subject to a Vegard's law correction. In the recent past, there have been definitive reviews of the structures of the synthetic[10,11] and mineral LDHs[12] supporting the cation-disordered structure model. Earlier DFT calculations have been performed on large supercells that were constructed to mimic the cation-disordered structure.[13,14]

The validity of the cation-disordered structure model critically depends on the degree of substitution of the divalent ion, x. For the limiting upper value of $x = 0.33$, Pauling's cation avoidance rule[15] precludes cation disorder and predicts a cation-ordered structure, in which the trivalent ion M'^{3+} is in an ordered arrangement relative to the divalent ions. The resulting supercell dimension is $a = \sqrt{3} \times a_o$ (ca. 5.35 Å). For lower values of x, both cation-ordered, as well as cation-disordered, structure models are envisaged.[16] For instance, for $x = 0.25$, which corresponds to the composition of a preponderance of mineral LDHs, cation ordering predicts a supercell with $a = 2 \times a_o$ (ca. 6.22 Å). At the same time, cation-disordered structures are also envisaged without violation of Pauling's cation avoidance rule.

Experimental work aimed at the precipitation of cation-ordered structures has primarily focused on LDHs with the composition of $x = 0.33$.[17] Evidence for cation ordering manifests itself in the form of weak supercell reflections, corresponding to the *100* and *101* planes of the enlarged unit cell in powder X-ray diffraction patterns. These structures have been refined

[a] *Department of Chemistry, Central College, Bangalore University, Bangalore 560-001, India*
E-mail: gangaperiyasamy@gmail.com

Supporting information and ORCID(s) from the author(s) for this article are available on the WWW under https://doi.org/10.1002/ejic.201700716.

within the space group $P\bar{3}$ ($a \approx 5.35$ Å, $c \approx 11.5$ Å). They are the [Zn–Al],[18] [Cu–Cr],[17] and the [Zn–Cr][19] LDHs. All of these LDHs have SO_4^{2-} ions in the interlayer. It is likely that the SO_4^{2-} ions assist the ordered stacking of the metal hydroxide layers.[20,21] From the value of the *c* parameters, it is evident that all of these three LDHs crystallize in the structure of a one-layer polytype of hexagonal symmetry (1H). The following consequences of cation ordering are noted:

(i) The ideal crystal symmetry $R\bar{3}m$ of the (pseudo) single-cation structure is reduced to $P\bar{3}$.

(ii) The 2D array of the hydroxy ions is non-uniformly distended, leading to the loss of hexagonal symmetry.

(iii) The $[M(OH)_6]$ (M = Cu^{2+}, Zn^{2+}) coordination symmetry is lowered from the ideal D_{3d} to C_3 (or ca. C_{3v}), whereas the coordination symmetry of $[M'(OH)_6]$ (M′ = Al^{3+}, Cr^{3+}) is preserved as D_{3d}, which is expected for the single-cation structure.[17]

Cation ordering lowers the symmetry at all levels of the structural hierarchy compared with the (pseudo) single-cation structure. This paper examines the electronic structure of the cation-ordered LDH.

Results and Discussion

Computation of the Structure by Energy Minimization

All of the three LDHs crystallize in hexagonal symmetry (space group $P\bar{3}$; a_{obs} = 5.35–5.41 Å, c_{obs} = 11.05–11.15 Å; obs: observed).[17–19] These structures were used as input for the SIESTA program. The experimental structures were obtained from X-ray diffraction data and do not include proton positions. The protons were added on the basis of the O–H bond lengths. The O–H bonds of the intercalated water molecules were oriented in the direction of the sulfate ions, maintaining a suitable antibump distance. The protons belonging to the hydroxy groups of the metal hydroxide layer were oriented perpendicular to the metal hydroxide layer.

Energy minimization was carried out without imposition of any symmetry constraints. The computed cell parameters (Table 1) show that in all of the LDHs, the cell angles depart from the ideal values ($\alpha = \beta = 90°$; $\gamma = 120°$) by < 3 %. The computed cell edges a_{comp} and b_{comp} (comp: computed) differ from one another by < 3 % in the Zn-containing LDHs. The larger variation seen in the [Cu–Cr] LDH (ca. 6 %) is also within

Table 1. Computed structural parameters of the [Zn–Al], [Cu–Cr], and [Zn–Cr] LDHs. The observed values obtained from diffraction studies are in parentheses.[a]

Structural parameters	M^{2+} = Zn; M^{3+} = Al	M^{2+} = Cu; M^{3+} = Cr	M^{2+} = Zn; M^{3+} = Cr
a [Å]	5.564 (5.348)	5.729 (5.408)	6.028 (5.414)
b [Å]	5.643 (5.348)	5.394 (5.408)	5.861 (5.414)
c [Å]	11.439 (11.153)	11.806 (11.055)	12.817 (11.070)
α [°]	91.52 (90)	90.52 (90)	87.29 (90)
β [°]	91.68 (90)	89.12 (90)	92.30 (90)
γ [°]	120.56 (120)	118.66 (120)	120.21 (120)
M^{2+}–O1 [Å]	2.317–2.218 (2.211, 2.110)	2.186–2.094 (2.132, 2.034)	2.262–2.101 (2.063, 2.041)
M^{3+}–O1 [Å]	1.961–1.916 (1.788)	1.976 (1.902)	1.931–1.886 (1.907)
S–O_a [Å]	1.484 (1.412)	1.525 (1.328)	1.478 (1.229)
S–O_b [Å]	1.598 (1.660)	1.543 (1.380)	1.504 (1.393)

[a] [Zn–Al],[17] [Cu–Cr],[16] [Zn–Cr].[18]

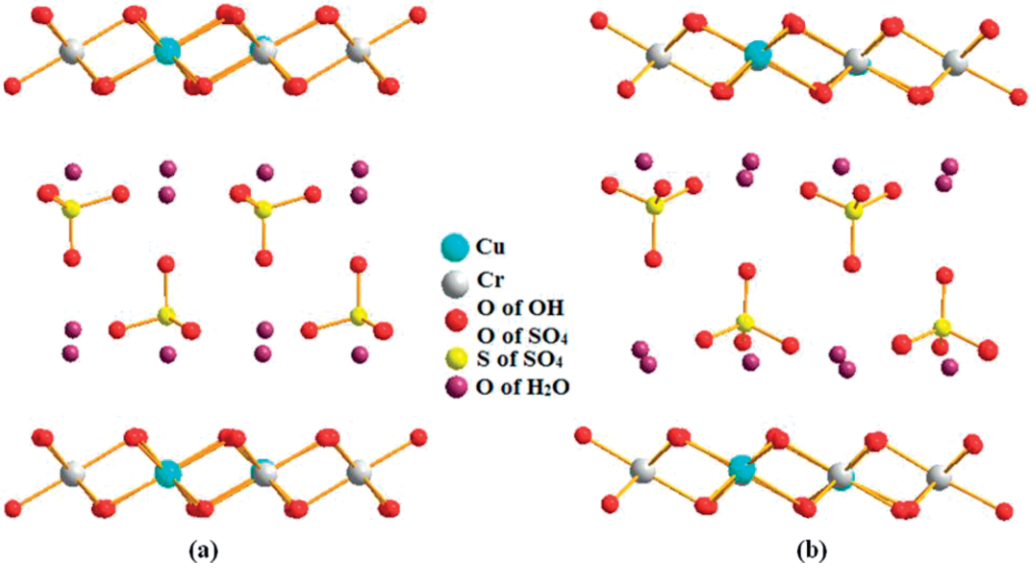

Figure 1. Comparison of (a) the observed with (b) the computed structure of the [Cu–Cr] LDH. The hydrogen atoms are deleted in (b) to facilitate comparison.

the acceptable range. The computed structure is therefore approximately hexagonal. A comparison of the computed with the observed structures offers a good visual match (Figure 1, Figures S1–S2).

The observed structure has a single M'^{3+}–OH bond length and two M^{2+}–OH bond lengths. The absence of any symmetry constraints on the computation yields six different values for the two bond lengths. The range of computed values (Table 1) matches the observed values within acceptable limits. As the observed structures were obtained by the refinement of X-ray diffraction data, there are no proton positions. The computed proton positions therefore provide valuable information. The O–H bond lengths vary over a narrow range {0.984–1.015 Å in [Zn–Al]; 0.992–1.021 Å in [Cu–Cr]; 0.969–1.021 Å in [Zn–Cr]}; all of the hydroxy groups are chemically similar, and each OH group is coordinated to two M^{2+} cations and one M'^{3+} cation.

A close look at the local coordination symmetry of the metal ions (Table 2) is revealing. In the observed structures, the [M′(OH)$_6$] (M′ = Al^{3+}, Cr^{3+}) polyhedra have D_{3d} point-group symmetry. In the computed structures, the D_{3d} point-group symmetry is retained in the [Zn–Al] LDH. The [Cr(OH)$_6$] polyhedron has D_{2h} symmetry in the [Cu–Cr] LDH, and C_{3v} symmetry in the [Zn–Cr] LDH. In the observed structures, the [M(OH)$_6$] polyhedra have C_3 symmetry when M = Cu^{2+},[22] and D_3 symmetry when M = Zn^{2+}.[23] In the computed structures, the coordination symmetry of the [Cu(OH)$_6$] polyhedron varies from C_s to C_2 and that of the [Zn(OH)$_6$] polyhedron is D_3 and C_2. The lowering of the coordination symmetry of the divalent ions from the ideal D_{3d} is especially puzzling in crystals of high symmetry, and it forms the subject matter of this paper. Reduction in the coordination symmetry eliminates the degeneracy of local MOs, leading to a variation in the density of states (DOS). To the extent that our computation predicts this lowering of symmetry, it should also reveal the underlying electronic factors that cause the distortion.

Table 2. Point-group symmetry of the metal-coordination polyhedra computed by the SYMGROUP program for the optimized structures.

[Zn–Al] LDH			
[Zn(OH)$_6$]		[Al(OH)$_6$]	
Point group	Accepted scores	Point group	Accepted scores
D_3	0.03–0.08	D_{3d}	0.005–0.05
[Cu–Cr] LDH			
[Cu(OH)$_6$]		[Cr(OH)$_6$]	
Point group	Accepted scores	Point group	Accepted scores
C_2	0.01–0.07	D_{2h}	0.01–0.09
C_s	0.05–0.07		
[Zn–Cr] LDH			
[Zn(OH)$_6$]		[Cr(OH)$_6$]	
Point group	Accepted scores	Point group	Accepted scores
C_2	0.05–0.09	C_{3v}	0.02–0.08

Band Gap

The band gap is a reflection of the thermodynamic stability of the LDH. The band gaps obtained from the SIESTA program are 3.29 eV [Zn–Al], 0.29 eV [Cu–Cr], and 0.07 eV [Zn–Cr] for the three LDHs (Figure 2). The LDHs are high-band-gap insulators, and computed band gaps are underestimated in the [M–Cr] (M = Cu, Zn) LDHs. There are two possible reasons:

(i) The use of a localized molecular basis set.

(ii) The exchange correlation potentials fails to account for the electronic correlation.

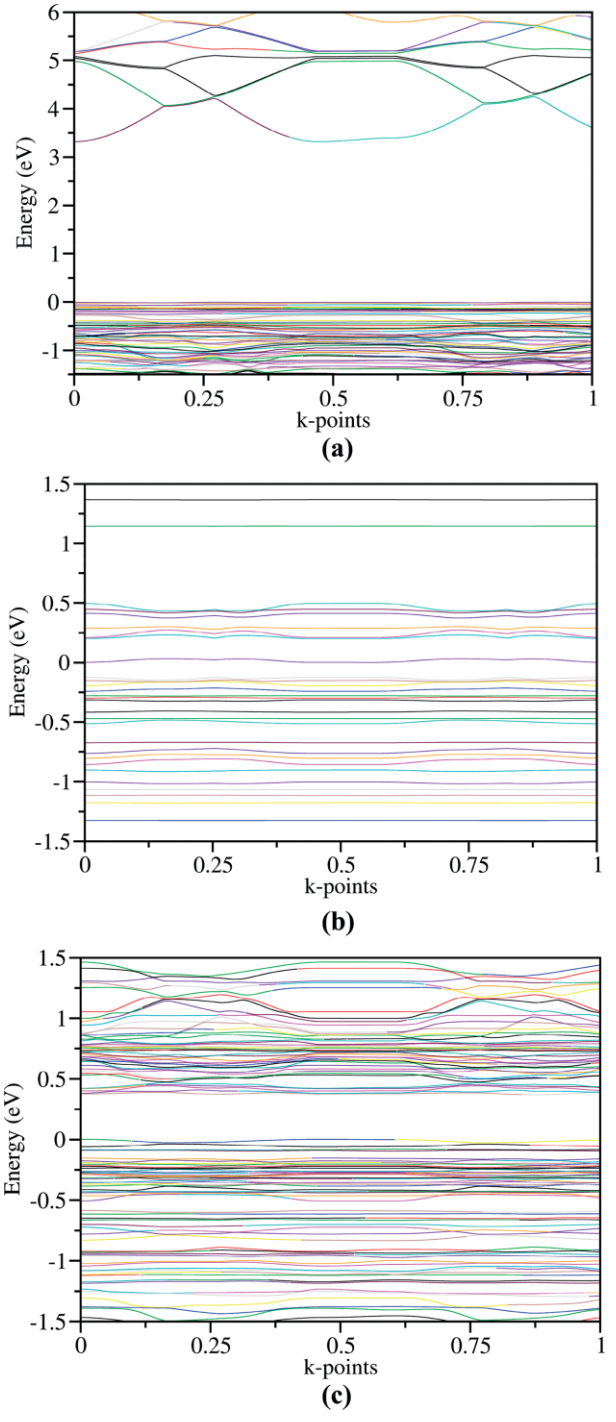

Figure 2. Band gaps obtained from the SIESTA program for: (a) [Zn–Al], (b) [Cu–Cr], and (c) [Zn–Cr] LDHs.

The latter aspect is not significant for the [Zn–Al] LDH, as Zn^{2+} has a filled d-shell, and Al^{3+} has no d-electrons. Consequently, the band gap predicted for the [Zn–Al] LDH is consist-

ent with the insulating nature of the LDH. In the [Cu–Cr] LDH, both metal ions have incomplete d-shells, and in [Zn–Cr], Cr^{3+} has an incomplete d-shell, leading to the underestimation of the band gap in these two cases. To resolve this, the plane-wave basis set and the hybrid functional PBE in the plane-wave SCF code, as implemented in the Quantum Espresso package, was used to recompute the electronic structure for the optimized crystal structure. The revised band gaps of 0.25 eV [Zn–Al], 0.72 eV [Cu–Cr], and 0.03 eV [Zn–Cr] for the LDHs were still far from satisfactory.

A Hubbard term (U_{eff}) was added to effectively account for the electronic correlation. The band gaps realized after adding U_{eff} were 3.04 eV [Zn–Al], 2.19 eV [Cu–Cr], and 2.62 eV [Zn–Cr] (Figure S3). The Hubbard term introduced the band gap into the [M–Cr] (M = Cu^{2+}, Zn^{2+}) LDHs, while at the same time, it moderated the value for the [Zn–Al] LDH. The opposing effects of U_{eff} on the two types of LDHs lends confidence to the computation. Moreover, the contributions of different atomic orbitals at the Fermi level follow the same trend in both methods (Table S4). Therefore, the band structures in Figure 2 are used in further discussions.

Density of States

Electronic-Structure Basis for the Distortion of the [M(OH)$_6$] (M = Cu^{2+}, Zn^{2+}) Polyhedron

One of the significant structural features that distinguishes a cation-ordered structure is the reduction in the symmetry of the [M(OH)$_6$] polyhedron. In a (pseudo) single-cation structure model, which describes a cation-disordered structure, the idealized coordination symmetry around the metal ions is D_{3d}.[17] We ask the question: What are the possible factors underlying the observed distortion? Three distortion models can be envisaged, each of which has a distinctive signature on the electronic structure of the LDH.

(i) Jahn–Teller Effect: Jahn–Teller distortion of the metal-ligand polyhedron occurs when there is a degenerate ground state; it is well known for d^4 and d^9 systems with octahedral symmetry. The d^9 configuration yields a degenerate ground state, even in D_{3d} coordination symmetry, wherein the d-orbitals transform as e_g ($d_{x^2-y^2}$, d_{xy}) < a_{1g} (d_{z^2}) < e_g (d_{xz}, d_{yz}) in increasing order of energy. The distortion of the D_{3d} symmetry is less well known, and as we have argued earlier,[17] the stepwise dis-

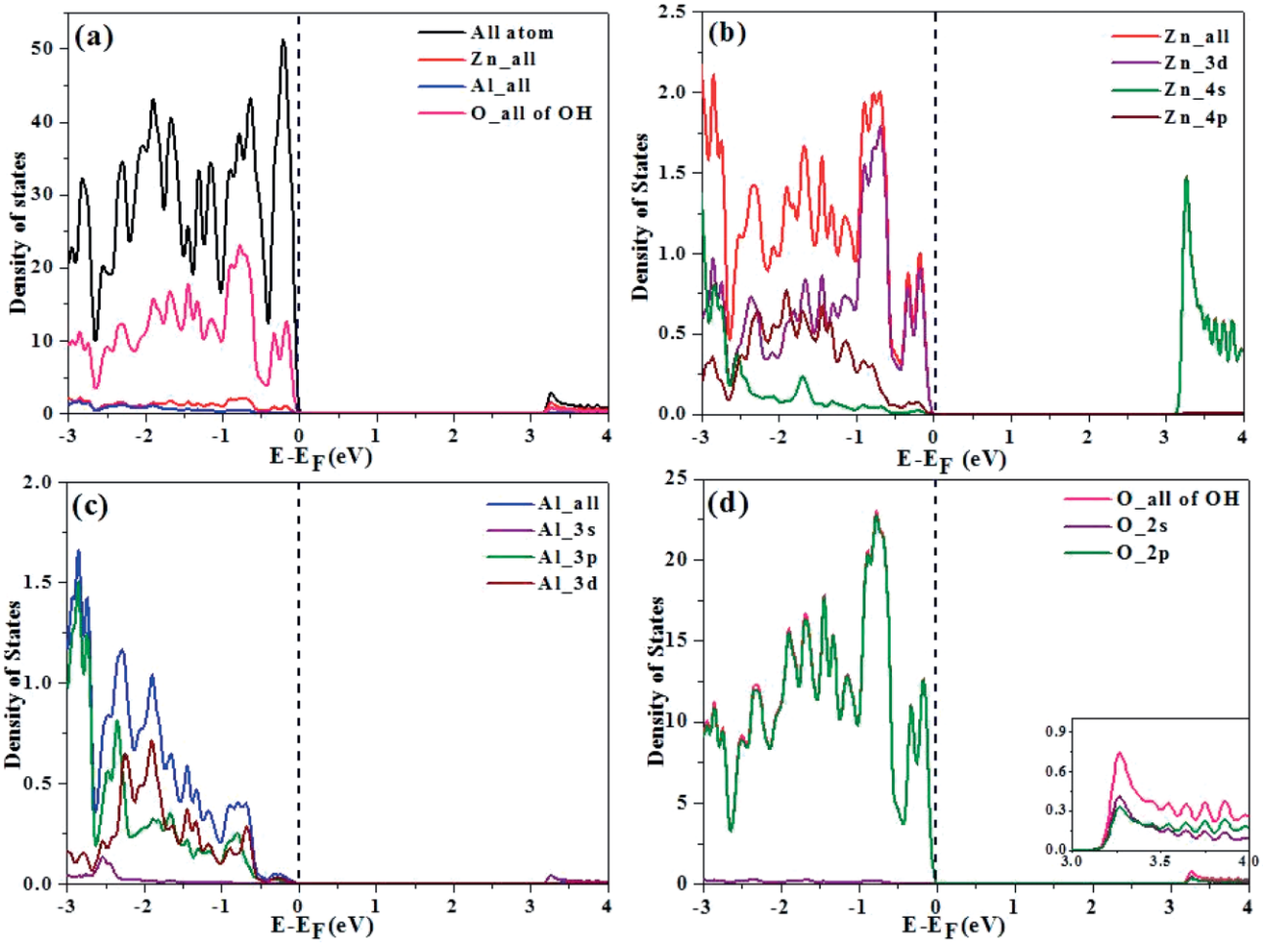

Figure 3. (a) Total density of states for [Zn–Al] LDH. The partial DOS due to (b) Zn, (c) Al, and (d) O, together with the orbital contributions, are shown. The Fermi level is indicated by vertical dashed lines. The inset in (d) highlights the contribution of the O-orbitals to the CB.

tortion of $D_{3d} \rightarrow C_{3v} \rightarrow C_3$ results in a nondegenerate ground state only when the coordination symmetry is C_3. The lifting of the degeneracy should result in a significant d-contribution to both the valence band (VB) and the conduction band (CB) of the LDH.

(ii) 2D Peierls-Type Distortion: In a (pseudo) single-cation structure, the OH^- ions are arranged in a hexagonal array, and the metal atoms occupy alternative layers of six-coordinate sites. In a perfect 2D array of OH^- ions, all of the O(2p) levels are degenerate, and no distortion is expected if the O(2p) states are fully occupied. This would be the case in the limits of pure ionic bonding, but partial covalency of the bonding within the metal hydroxide layers results in partial filling of the O(2p) states. In such a situation, a Peierls-type distortion of the hexagonal array of OH^- ions would lift the degeneracy and open up a gap between the O(2p) states, lending stability to the structure. In such an instance, both the VB and the CB are expected to have a significant O(2p) contribution.

(iii) Packing Considerations: The divalent and trivalent ions differ considerably in their radii. The LDH structure is highly flexible, and ions with widely different radii, including those exceeding the traditional tolerance limits imposed by the Hume–Rothery criteria, coprecipitate as single-phase LDHs. In such an eventuality, packing considerations, induced by the choice of the space group of the structure model used for refinement, can generate an apparent loss in metal-coordination symmetry.

We examine which of these distortion models apply to the title LDHs, by examining their total and partial density of states.

[Zn–Al] LDH

The conduction-band DOS is much smaller than that of the valence band. The major contribution to the CB is from Zn (4s) (Figure 3), which is unsurprising, as electrons from Zn(4s) are expected to be transferred to O(2p) levels due to bonding within the metal hydroxide layer. The CB also has a significant contribution from the O(2p) levels of the OH^- species, showing that this electron transfer is inadequate to generate fully filled OH^-–O(2p) levels, suggesting considerable covalency in the bonding within the metal hydroxide layer. The holes residing on the OH^-–O(2p) levels are therefore due to the covalency of the Zn–O bonds within the metal hydroxide layers.

The absence of any Zn(3d) contribution to either the VB or the CB rules out the role of Jahn–Teller-like effects in the distortion of the $[Zn(OH)_6]$ polyhedron. The significant contribution of the OH^-–O(2p) levels in both the VB and the CB is supportive of a 2D Peierls-type distortion effect.

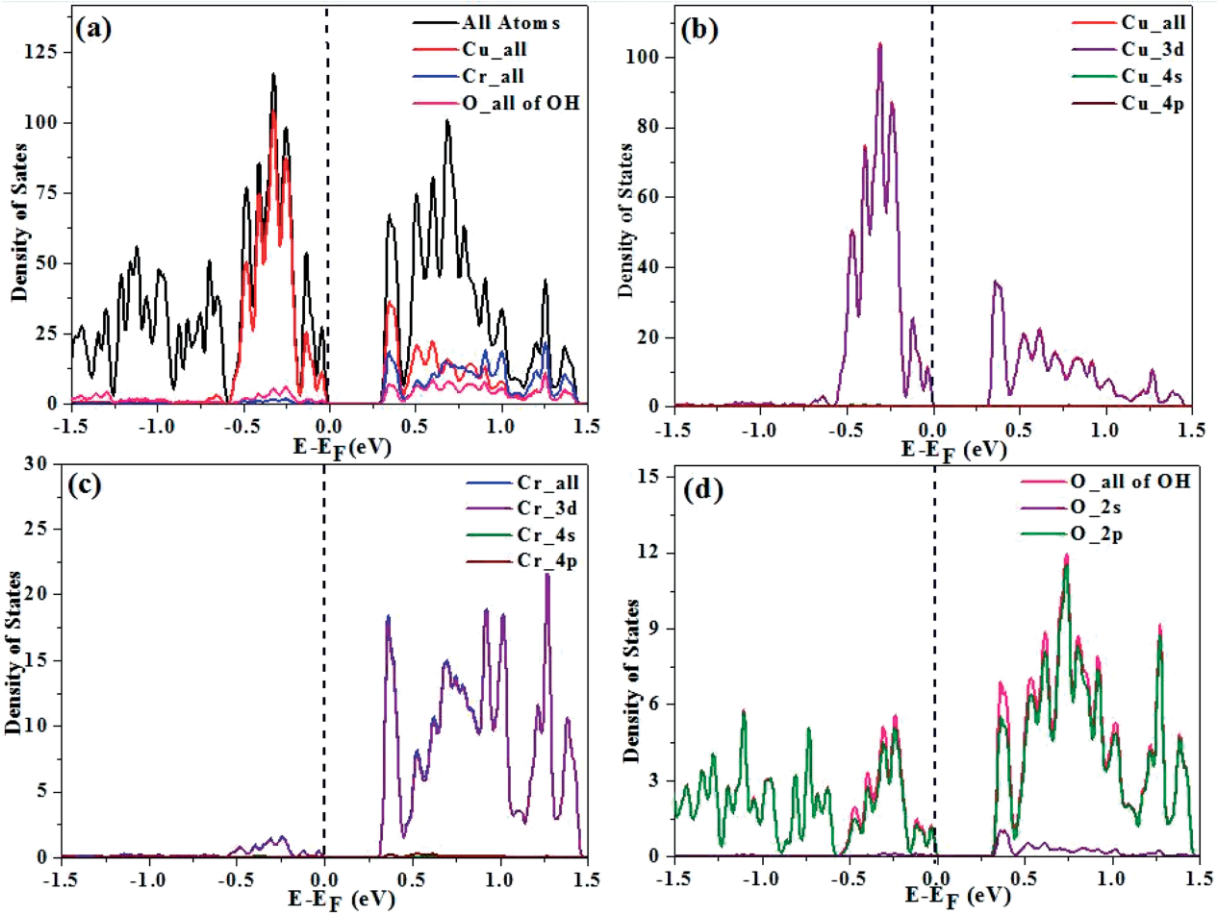

Figure 4. (a) Total density of states for [Cu–Cr] LDH. The partial DOS due to (b) Cu, (c) Cr, and (d) O, together with the orbital contributions, are shown. The Fermi level is indicated by vertical dashed lines.

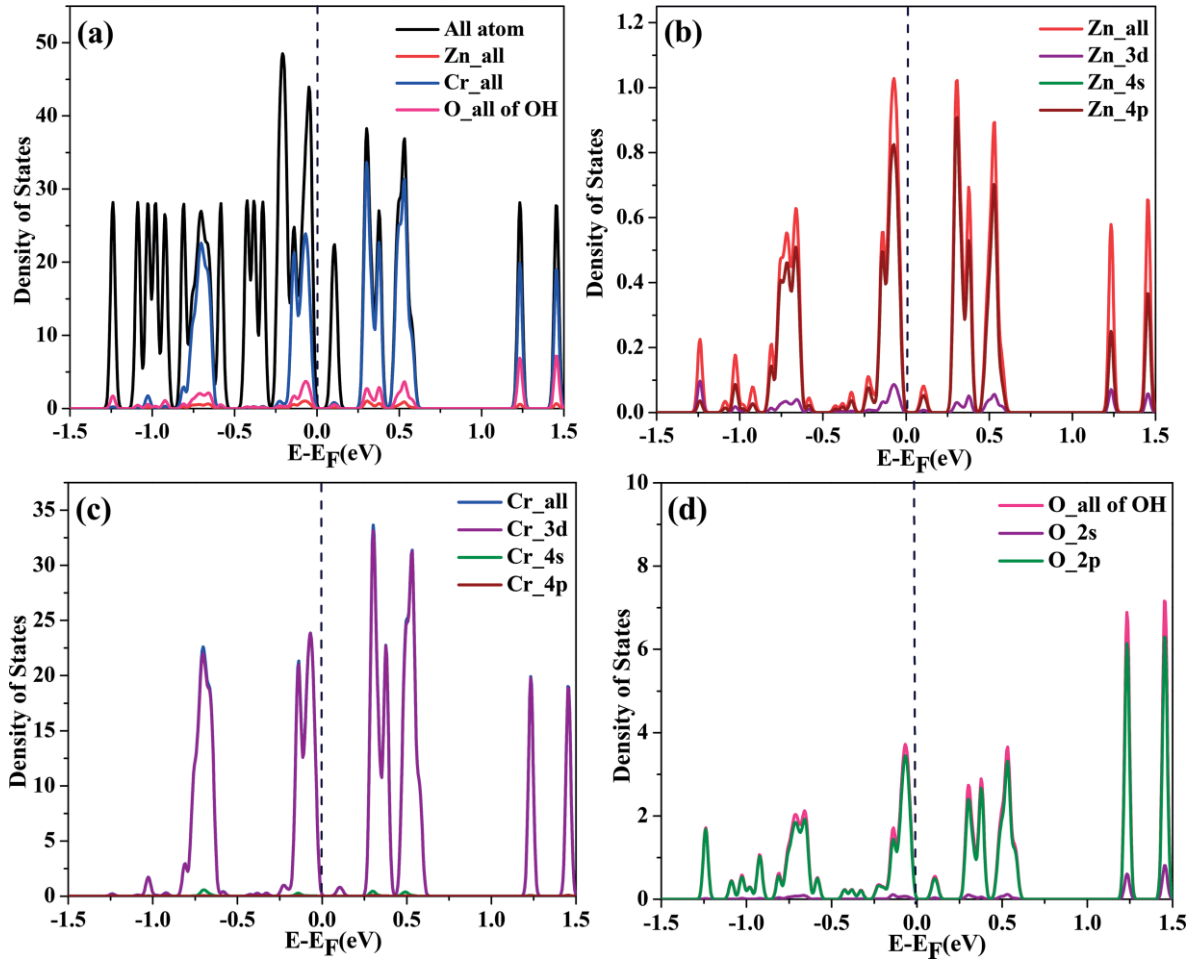

Figure 5. (a) Total density of states for [Zn–Cr] LDH. The partial DOS due to (b) Zn, (c) Cr, and (d) O, together with the orbital contributions, are shown. The Fermi level is indicated by vertical dashed lines.

[Cu–Cr] LDH

The DOS at the bottom of the CB has a major contribution from Cu(3d) and, as expected, a contribution from Cr(3d) as well. The top of the VB is dominated by Cu(3d) (Figure 4). Notably, there is a near absence of any OH^-–O(2p) contribution to both the VB and the CB. The significant contribution of the Cu(3d) levels to both the VB and the CB indicates the Jahn–Teller effect is the underlying reason for the distortion of the $[Cu(OH)_6]$ polyhedron.

[Zn–Cr] LDH

The bottom of the CB and the top of the VB have major contributions from Cr(3d) (a non-Jahn–Teller ion) and an absence of OH^-–O(2p) and Zn(3d) (Figure 5). The electronic-structure calculations do not predict any distortion in the $[Zn(OH)_6]$ polyhedron because of the absence of the Zn(3d) and the OH^-–O(2p) contributions to both the VB and the CB. The observed structure reports minimal distortion in the $[Zn(OH)_6]$ polyhedron compared with the divalent polyhedra in the [Cu–Cr] and [Zn–Al] LDHs. The Zn^{2+} and Cr^{3+} ions, with different radii, form metal-coordination polyhedra of different sizes. Packing these differently sized polyhedra within the layer induces the distortion. It appears that packing considerations are underlying the distortion of the $[Zn(OH)_6]$ polyhedron in the [Zn–Cr] LDH.

The intercalated SO_4^{2-} ions have no role in mediating the distortion of the metal coordination. Their role is to balance the positive charge of the metal hydroxide layer. The intercalated water molecules form a strong hydrogen-bonded network in the interlayer gallery to facilitate the charge distribution, which is otherwise centered at the trivalent cations.

Conclusion

The proposal of a cation-ordered structure model for LDHs is based on sound crystal chemical considerations, as envisaged by Pauling's cation avoidance rule. This model predicted a low coordination symmetry for the divalent cations, although the crystal symmetry itself is hexagonal. The structure model raised the important question: Is the lowering of the coordination symmetry an artifact of the space group employed for structure refinement, or are there more fundamental electronic factors that contribute to the lowering of the total energy of the crystal? This paper shows that the origin of the distortion in the coordination symmetry of the Cu^{2+} ion is Jahn–Teller distortion, but the distortion observed in the coordination symmetry of

Zn^{2+} in the [Zn–Al] LDH has a 2D Peierls-type origin. The [Zn–Cr] LDH structure is probably driven by the choice of the space group and is purely an artifact of the packing together of cations of different ionic radii.

Computational Section

The models for the calculations were generated on the basis of the reported crystal structures for [Zn–Al], [Cu–Cr], and [Zn–Cr] LDHs.[17,18] The cell size ($2\sqrt{3} \times 2\sqrt{3}$) R30° was chosen with proper three-dimensional periodic boundary conditions for the calculation. The interlayer sulfates were modeled on the basis of layer charges reported experimentally, while the water molecules were modeled on the basis of TGA results. The three models, thus generated, were optimized using DFT methods, as implemented in the SIESTA package,[24] which consists of localized molecular-orbital basis sets. All atoms are represented with the Troullier–Martins norm, conserving pseudopotentials in the Kleinman–Bylander form, together with the gradient-corrected Perdew, Burke, and Ernzerhof (PBE) exchange correlation functional.[25] A double-*z* basis (DZP)[26] set with polarization orbitals was included for all atoms, together with a real-space mesh cut-off of 300 Ry. The Grimme-D2 dispersion correction[27] was included to describe long-range interactions. All models were geometry-optimized without imposing any symmetry constraints, and the interatomic force was relaxed up to 0.01 eV $Å^{-1}$. The atomic coordinates were adjusted without any symmetry constraints, with convergence criteria of 0.05 eV for energy and 0.05 Å for displacement. The Cartesian coordinates of all of the atoms in the optimized structures are reported in Table S5. The sampling of the Brillouin zone was done with $3 \times 3 \times 50$ *k*-point grids. Bands, the density of states, and the projected density of states were calculated at the same *k*-point grid in hexagonal symmetry. Further, the optimized structures were validated as minima by computing the vibrational frequencies on the basis of phonon calculations at the γ-point, using the SIESTA package, by central finite differencing of the analytical first derivatives, with a displacement of 0.04 Bohr (Table S6).

In each case, the optimized geometry was used to calculate the electronic properties using the PWSCF (plane-wave self-consistent field) code within the generalized gradient approximation (GGA) and Perdew–Burke–Ernzerhof (PBE) functional, as implemented in the QUANTUM ESPRESSO Package.[28] The plane-wave basis set of 0.01 Ryd, with Marzari–Vanderbilt smearing, was used to describe valence electrons with a kinetic energy cutoff up to 24 Ryd (convergence tests with 28 Ryd). Ionic cores are described by the ultrasoft pseudopotential.[29] The *k*-point mesh and cell size are also maintained at the plane-wave basis set. The following convergence criteria were used for structure optimization and energy calculations: difference of the total energies of last two consecutive steps was less than 10^{-6} Ryd, and the total force was less than 0.002 Ryd $Bohr^{-1}$. The following Hubbard U_{eff} potentials of (i) 12 eV for the 3d orbitals of Cu^{2+}, Zn^{2+}, and Cr^{3+}, (ii) 6.5 eV for the 2p orbitals of oxygen, and (iii) 8.5 eV for the 3p orbitals of Al^{3+} were used for the calculation in order to obtain appropriate band gaps. These U_{eff} values were based on linear-response theory[30,31] and have been successfully used in earlier computations of LDH systems.[14]

The coordination symmetry of the metal ions was computed using the SYMGROUP program.[32] The Cartesian coordinates of the six closest hydroxy O-atoms around each of the metal ions were used as input for the SYMGROUP program. A score was generated for each of the possible symmetry elements, such as C_n (n = 1–6), mirror plane (*r*), and inversion point (*i*). A score = 0 suggested exactness of the symmetry. A score higher than zero showed departure from ideal symmetry. In all of the computations reported in this paper, owing to the numerical difference in the atomic positions, none of the computed scores were zero. However, many symmetry elements had scores which were nonzero, but very low, typically 10^{-2}–10^{-3}. These symmetry elements were accepted, and the approximate coordination symmetry was deduced. The cell used for the computation of the electronic structure was comprised of eight M^{2+} ions and four M'^{3+} ions. In the observed structure, all of the divalent ions had the same coordination. The computed structure was obtained without the application of any symmetry restraints. Consequently, each of the twelve cations within the supercell had a slightly different coordination, defined by unequal bond lengths and bond angles. To compute the coordination symmetry, four divalent and two trivalent cations were chosen randomly in each LDH to evaluate the range of coordination symmetries adopted.

Supporting Information (see footnote on the first page of this article): Comparison of (a) the observed with (b) the computed structures of [Zn–Al] LDH and [Zn–Cr] LDH; revised band gaps obtained after adding the Hubbard term into the plane-wave basis set for (a) the [Zn–Al], (b) the [Cu–Cr], and (c) the [Zn–Cr] LDHs; Cartesian coordinates of all of the atoms in the optimized structure of the [Zn–Al], [Cu–Cr], and [Zn–Cr] LDHs; computed ($3N$ – 6) frequencies [cm^{-1}] for the optimized structures of the [Zn–Al], [Cu–Cr], and [Zn–Cr] LDHs.

Acknowledgments

G. P. thanks the University Grants Commission – Faculty Recharge Programme (UGC-FRP), Government of India (GOI), for financial support. K. J. thanks the Council of Scientific Industrial Research (CSIR), GOI, for the award of a Senior Research Fellowship (SRF). P. V. K. is the recipient of a Ramanna Fellowship of the Department of Science and Technology (DST), GOI.

Keywords: Cation ordering · Density functional calculations · Jahn–Teller distortion · 2D "Peierls"-type distortion · Electronic structure

[1] D. G. Evans, X. Duan, *Chem. Commun.* **2006**, 485–496.
[2] A. Matei, R. Birjega, A. Nedelcea, A. Vlad, D. Colceag, M. D. Ionita, C. Luculescu, M. Dinescu, R. Zavoianu, O. D. Pavel, *Appl. Surf. Sci.* **2011**, *257*, 5308–5311.
[3] Z. P. Xu, J. Zhang, M. O. Adebajo, H. Zhang, C. Zhou, *Appl. Clay Sci.* **2011**, *53*, 139–150.
[4] S. V. Prasanna, R. A. P. Rao, P. V. Kamath, *J. Colloid Interface Sci.* **2006**, *304*, 292–299.
[5] S. V. Prasanna, P. V. Kamath, *J. Colloid Interface Sci.* **2009**, *331*, 439–445.
[6] L. Lv, J. He, M. Wei, X. Duan, *Ind. Eng. Chem. Res.* **2006**, *45*, 8623–8628.
[7] L. Lv, Y. Wang, M. Wei, J. Cheng, *J. Hazard. Mater.* **2008**, *152*, 1130–1137.
[8] J. Zhou, Z. P. Xu, S. Qiao, Q. Liu, Y. Xu, G. Qian, *J. Hazard. Mater.* **2011**, *189*, 586–594.
[9] W. T. Reichle, *Solid State Ionics* **1986**, *22*, 135–141.
[10] I. G. Richardson, *Acta Crystallogr., Sect. B: Struct. Sci. Cryst. Eng. Mater.* **2013**, *69*, 150–162.
[11] I. G. Richardson, *Acta Crystallogr., Sect. B: Struct. Sci. Cryst. Eng. Mater.* **2013**, *69*, 414–417.
[12] S. J. Mills, A. G. Christy, J.-M. R. Génin, T. Kameda, F. Colombo, *Mineral. Mag.* **2012**, *76*, 1289–1336.
[13] H. Yan, M. Wei, J. Ma, D. G. Evans, X. Duan, *J. Phys. Chem. A* **2010**, *114*, 7369–7376.
[14] P. I. R. Moraes, S. R. Tavares, V. S. Vaiss, A. A. Leitão, *J. Phys. Chem. C* **2016**, *120*, 9965–9974.

[15] L. Pauling, *J. Am. Chem. Soc.* **1929**, *51*, 1010–1026.
[16] W. Hofmeister, H. V. Platen, *Cryst. Rev.* **1992**, *3*, 3–26.
[17] K. Jayanthi, P. V. Kamath, *Dalton Trans.* **2013**, *42*, 13220–13230.
[18] S. Radha, K. Jayanthi, J. Breu, P. V. Kamath, *Clays Clay Miner.* **2014**, *62*, 53–61.
[19] S. Radha, P. V. Kamath, *Inorg. Chem.* **2013**, *52*, 4834–4841.
[20] M. A. Cooper, F. C. Hawthrone, *Can. Mineral.* **1996**, *34*, 91–97.
[21] D. M. C. Huminicki, F. C. Hawthrone, *Can. Mineral.* **2003**, *41*, 79–82.
[22] K. Jayanthi, P. V. Kamath, *Cryst. Growth Des.* **2016**, *16*, 4450–4456.
[23] K. Jayanthi, S. Nagendran, P. V. Kamath, *Inorg. Chem.* **2015**, *54*, 8388–8395.
[24] J. M. Soler, E. Artacho, J. D. Gale, A. Garcia, J. Junquera, P. Ordejon, D. Sanchez-Portal, *J. Phys. Condens. Matter* **2002**, *14*, 2745–2779.
[25] J. P. Perdew, K. Burke, M. Ernzerhof, *Phys. Rev. Lett.* **1997**, *78*, 1396–1396.
[26] O. F. Sankey, D. J. Niklewski, *Phys. Rev. B* **1989**, *40*, 3979–3995.
[27] S. Grimme, *J. Comput. Chem.* **2006**, *27*, 1787–1799.
[28] P. Giannozzi, S. Baroni, N. Bonini, M. Calandra, R. Car, C. Cavazzoni, D. Ceresoli, G. L. Chiarotti, M. Cococcioni, I. Dabo, A. Dal Corso, S. Fabris, G. Fratesi, S. de Gironcoli, R. Gebauer, U. Gerstmann, C. Gougoussis, A. Kokalj, M. Lazzeri, L. Martin-Samos, N. Marzari, F. Mauri, R. Mazzarello, S. Paolini, A. Pasquarello, L. Paulatto, C. Sbraccia, S. Scandolo, G. Sclauzero, A. P. Seitsonen, A. Smogunov, P. Umari, R. M. Wentzcovitch, *J. Phys. Condens. Matter* **2009**, *21*, 395502–395521.
[29] The pseudopotentials (H.pbe-rrkjus.UPF, Al.pbe-rrkj.UPF) were generated by Andrea Dal Corso and downloaded from http://www.quantum-espresso.org (accessed January 21, 2014).
[30] A. Consiglio, Z. Tian, *Sci. Rep.* **2016**, *6*, 36875; https://doi.org/10.1038/srep36875.
[31] M. Cococcioni, S. de Gironcoli, *Phys. Rev. B* **2005**, *71*, 035105-1-16.
[32] D. Casanova, P. Alemany, S. Alvarez, *SYMOP*, Universidad de Barcelona, Barcelona, Spain, **2007**.

Received: June 16, 2017

